IJCRT.ORG ISSN: 2320-2882



# INTERNATIONAL JOURNAL OF CREATIVE RESEARCH THOUGHTS (IJCRT)

An International Open Access, Peer-reviewed, Refereed Journal

# Structural and Optical Characterization of Cu-Doped ZnO Nanoparticles Synthesized via Precipitation Method

#### Shashi Bhushan Rana

Associate Professor

Department of Engineering & Technology

Guru Nanak Dev University Regional Campus Gurdaspur (Punjab) India

Abstract: Zinc oxide (ZnO) is an II–VI semiconductor distinguished by its wide direct band gap of 3.37 eV and large exciton binding energy of 60 meV, making it a strong candidate for blue-to-ultraviolet optoelectronic devices. Here, we describe the synthesis of undoped and Cu-doped ZnO nanoparticles prepared through a straightforward precipitation route, followed by an extensive structural and optical investigation. X-ray diffraction (XRD) confirms that every sample crystallizes in the hexagonal wurtzite phase with no detectable secondary phases. Incorporating Cu<sup>2+</sup> ions (ionic radius 0.73 Å) in place of Zn<sup>2+</sup> (0.60 Å) slightly enlarges the lattice constants and decreases the average crystallite size, a consequence of lattice strain and inhibited grain growth. Scanning electron microscopy (SEM) reveals progressive particle agglomeration and grain coarsening at higher annealing temperatures, consistent with improved crystallinity. Energy-dispersive X-ray spectroscopy (EDS) verifies elemental purity and successful Cu incorporation. Optical properties, examined via UV-visible absorption and photoluminescence (PL) spectroscopy, show a quantum-confinement-induced blue shift in the band gap for smaller particles, while Cu doping introduces a red-shifted UV emission, confirming dopant integration into the ZnO lattice. PL spectra display near-band-edge ultraviolet emission alongside pronounced blue and green bands whose intensities depend on annealing temperature and dopant level. The green luminescence—especially strong after annealing at 700 °C—is attributed to oxygen vacancies and Cu-related defect states. Overall, our results demonstrate how Cu incorporation and thermal processing tailor the structural and optical characteristics of ZnO nanoparticles, underscoring their potential in optoelectronic, sensing, and luminescent applications.

Index Terms - Cu doping, SEM, XRD, PL spectra, UV-visible.

# I. INTRODUCTION

Zinc oxide (ZnO), an II–VI compound semiconductor, has attracted increasing attention due to its wide direct band gap of 3.37 eV at room temperature and a high exciton binding energy of 60 meV. These properties make it highly suitable for optoelectronic applications across the blue, violet, [1-5] and ultraviolet regions of the electromagnetic spectrum. In recent years, ZnO nanoparticles have emerged as promising materials for a wide range of applications, including solar energy conversion, varistors, luminescent devices, electrostatic dissipative coatings, transparent UV-blocking films, chemical sensors, and spintronic devices [6-8]. This is largely due to their unique electrical, optical, mechanical, and magnetic properties, which arise from quantum confinement effects at the nanoscale [9-12]. To effectively investigate and utilize these properties in both pure and doped ZnO nanoparticles, the selection of an appropriate synthesis technique is crucial. An ideal method should facilitate the substitutional incorporation of dopant ions into the ZnO lattice and ensure atomic-scale homogeneity without forming unwanted secondary phases or nanoclusters. Various synthesis approaches—such as thermal decomposition, chemical vapor deposition, sol-gel, spray pyrolysis, microemulsion techniques, and precipitation—have been widely explored to produce ZnO nanoparticles [13-15].

Among these, the precipitation method stands out due to its simplicity, cost-effectiveness, and scalability for large-scale production [16-20]. One of its key advantages is the ability to achieve uniform dopant dispersion within the host matrix at the atomic level. The objective of the present study is to synthesize phase-pure ZnO nanoparticles, both undoped and doped, using a direct precipitation method, and to carry out detailed structural analysis using techniques such as X-ray diffraction (XRD), energy-dispersive X-ray spectroscopy (EDS), and scanning electron microscopy (SEM).

# 2. Synthesis and structural characterization of the prepared (undoped) pure ZnO and Cu doped ZnO nanoparticles.

#### 2. 1 Experimental detail

A direct precipitation method was employed to synthesize both pure and doped ZnO nanoparticles. Zinc nitrate  $(Zn(NO_3)_2)$  and sodium hydroxide (NaOH) served as the primary precursors. An aqueous solution of metal nitrates was prepared by dissolving highpurity metals (99.999%) in concentrated nitric acid. Separately, a measured amount of NaOH was dissolved in deionized water and subsequently mixed with the zinc nitrate solution, resulting in the formation of white precipitates. These precipitates were thoroughly washed several times with deionized water, followed by ethyl alcohol, to eliminate any residual impurities. The resulting fine precipitate was dried in an oven at  $100\,^{\circ}\text{C}$  for 15 hours. The dried powder was then finely ground and calcined at two different temperatures— $500\,^{\circ}\text{C}$  and  $700\,^{\circ}\text{C}$ —for 4 hours. In this study, both undoped ZnO and Cu-doped ZnO ( $Zn_{1-x}T_xO$ , where T=Cu) nanoparticles were prepared. For the doped samples, stoichiometric amounts of copper nitrate were added to the zinc nitrate solution prior to the precipitation process. Phase purity of the synthesized powders was confirmed using X-ray diffraction (XRD), performed with Cu K $\alpha$  radiation at  $40\,^{\circ}\text{kV}$  and  $30\,^{\circ}\text{mA}$ , a time constant of  $0.5\,^{\circ}\text{s}$ , and a crystal graphite monochromator. An increase in the intensity of diffraction peaks with higher annealing temperatures indicated enhanced crystallinity.

Crystallite sizes were estimated from the broadening of XRD peaks using the Scherrer equation. D =  $0.9\lambda$  /  $\beta$  cos $\theta$  where D is the average crystallite size,  $\lambda$  is the wavelength of the X-ray radiation,  $\beta$  is the full width at half maximum (FWHM) of the diffraction peak (corrected for instrumental broadening), and  $\theta$  is the Bragg angle. The morphology and particle size of the calcined nanoparticles were further examined using scanning electron microscopy (SEM).

# 2.2. Results and Discussions for Cu doped ZnO nanoparticles

## 2.2.1 XRD study

# 2.2.2 XRD Analysis of Pure and Cu-Doped ZnO Powders

Figure 1 presents the representative X-ray diffraction (XRD) patterns of both pure and Cu-doped ZnO nano powders. For comparative purposes, the XRD spectrum of a commercially available pure ZnO nano powder is also included. Prominent diffraction peaks corresponding to the (100), (002), and (101) planes are clearly visible at  $2\theta$  values of  $31.72^{\circ}$ ,  $34.38^{\circ}$ , and  $36.22^{\circ}$ , respectively, indicating the crystalline nature of the samples.

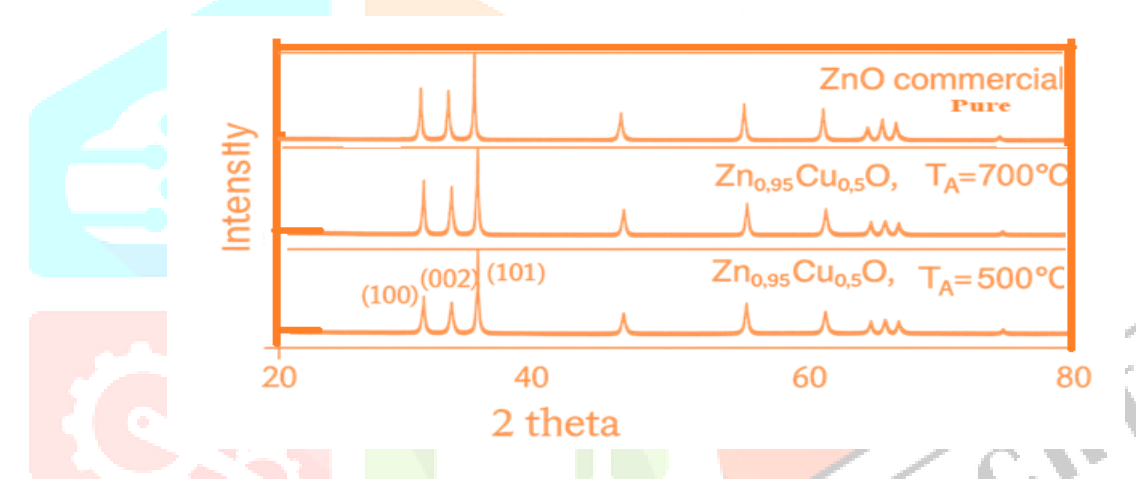


Fig.1 XRD of pure (commercial) and Cu doped ZnO nanoparticles

The average crystallite size, estimated using the Scherrer equation, was approximately 34 nm for pure ZnO. In comparison, Cudoped ZnO samples calcined at 500 °C showed reduced crystallite sizes of around 28 nm and 30 nm. The XRD data were further refined using the Rietveld method via the Rietica software, confirming a hexagonal wurtzite crystal structure with a P63mc space group for both pure and doped samples. Lattice parameters calculated from the XRD pattern of pure ZnO annealed at 700 °C were found to be a = 3.2475 Å and c = 5.2013 Å, closely matching standard reference values (a = 3.2488 Å, c = 5.2061 Å; JCPDS Card No. 36-1451). The absence of any additional diffraction peaks confirms the phase purity of the synthesized powders. For Cu-doped ZnO, a slight increase in lattice constants was observed, consistent with the substitution of Zn<sup>2+</sup> ions (ionic radius = 0.60 Å) by the larger Cu<sup>2+</sup> ions (ionic radius = 0.73 Å) in tetrahedral coordination. Additionally, a reduction in crystallite size was noted upon Cu incorporation, likely due to a suppressed sintering rate resulting from dopant atoms disrupting the crystal growth process.

# 2.2.3 SEM Analysis of Cu-Doped ZnO nanoparticles samples

Figure 2 shows scanning electron microscopy (SEM) images of Cu-doped ZnO nanoparticles calcined at 500 °C and 700 °C. At 500 °C, the particles appear agglomerated but uniformly distributed, with an average grain size of approximately 80 nm. Upon increasing the calcination temperature to 700 °C, the grain size increased to over 100 nm. This growth is attributed to enhanced crystallinity and neck formation between adjacent particles, driven by higher thermal energy.

It is important to note that grain sizes obtained from SEM and XRD differ significantly. SEM measures the physical grain boundaries visible on the particle surface, while XRD estimates the coherent diffracting crystalline domains, which are typically smaller.

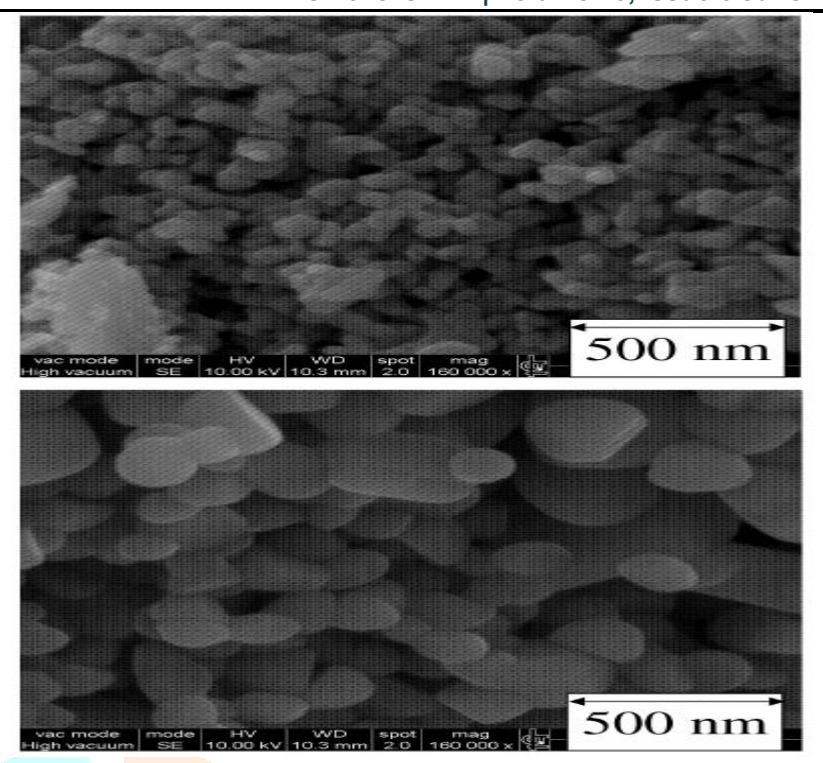


Figure 2: SEM Image of cu doped ZnO nano-sized particles. Top: ZnO, T<sub>A</sub> =500°C; Bottom: ZnO, T<sub>A</sub>=700°C. T<sub>A</sub> represents annealing temperature.

The SEM images further confirm the homogeneity of the doped samples, indicating uniform dispersion of Cu within the ZnO matrix without the formation of separate dopant phases. Therefore, the XRD measurements led to smaller size. The SEM images of doped samples indicate that the samples were homogeneous with dopants (Cu) substituting Zn sites in ZnO compound and do not contain any other dopant dominating phases.

- 3. Optical study of prepared pure ZnO and doped (Cu) ZnO nanoparticles
- 3.1 Optical characterization of the prepared (undoped) pure ZnO nanoparticles and doped (Cu) ZnO nanoparticles.

The optical characteristics and underlying processes in ZnO nanoparticles have been extensively studied for several decades. Owing to its wide direct band gap of 3.37 eV at room temperature and a high exciton binding energy of 60 meV, ZnO is regarded as a highly promising photonic material for applications in the blue to ultraviolet (UV) spectral range. Various experimental techniques—such as optical absorption, reflection, transmission, and photoluminescence (PL) spectroscopy—have been employed to investigate the optical behaviour of ZnO. In the present study, we focused specifically on analysing the optical properties of Cudoped ZnO nanoparticles using two primary techniques: UV-Visible (UV-Vis) absorption spectroscopy and photoluminescence spectroscopy. The optical properties of ZnO nanoparticles become increasingly significant as the particle size is reduced to the nanometer scale. When the particle size approaches the exciton Bohr radius (~1.8 nm for ZnO), quantum confinement effects begin to dominate, leading to a noticeable increase in the band gap. This phenomenon alters the material's optical transitions, including absorption and emission behaviours. Our UV-Vis absorption studies revealed such changes in both pure and Cu-doped ZnO samples, highlighting the impact of particle size and surface states on the band structure.

Additionally, PL spectra of nearly all synthesized ZnO samples exhibited strong near-band-edge (NBE) UV emission, accompanied by pronounced visible luminescence. These emissions are significantly influenced by the quality and nature of the nanoparticle surface. Numerous studies have demonstrated a close correlation between visible luminescence and the surface states of colloidal ZnO nanoparticles. However, a complete understanding of the mechanisms behind photoluminescence and the factors governing emission efficiency remains an ongoing challenge.

#### 3.2 Introduction to Cu Doping in ZnO

Doping is a well-established method to tailor the electrical and optical properties of semiconductors. In the case of ZnO, copper (Cu) doping has proven effective in modifying photoluminescent behavior by introducing localized defect levels or impurity states within the band gap. Cu acts as an acceptor in the ZnO lattice, with an energy level located approximately 0.17 eV below the conduction band minimum. This characteristic makes Cu a strong candidate for achieving p-type conductivity in ZnO, which is otherwise difficult to realize. Moreover, Cu incorporation affects luminescence by introducing extrinsic defect levels, thereby enabling tunability in optical emission properties for applications in optoelectronic and sensing devices.

## 3.2 Photoluminescence study of prepared pure ZnO and Cu doped ZnO Nanoparticles

# 3.2.1 Photoluminescence (PL) Analysis of Pure and Cu-Doped ZnO Nanoparticles

The photoluminescence (PL) spectra of both pure and Cu-doped ZnO nanoparticles, synthesized at two different annealing temperatures (500°C and 700°C), are presented in Figure 3. The PL spectrum of pure ZnO nanoparticles exhibits a strong ultraviolet (UV) emission peak at 377 nm, attributed to excitonic recombination near the band edge. In addition, broad visible emissions are observed with distinct peaks at 444 nm, 459 nm, 484 nm, and 524 nm. These emissions correspond to blue and green regions of the visible spectrum. The blue emission is divided into two components: (1) Band-I (444–459 nm): This emission diminishes in intensity

as annealing temperature increases and is primarily associated with interstitial zinc ( $Zn_i$ ) defects. Band-II (484–486 nm): Attributed to the direct recombination of electrons in the Zn 3d conduction band with holes in the 2p valence band. This emission may also result from oxygen antisite defects (2) Green emission (500–530 nm): This is generally due to recombination between a shallowly trapped electron and a deeply trapped hole, typically within oxygen vacancy centres.

## 3.2.2 PL Behaviour of Cu-Doped ZnO Nanoparticles at 500°C

For Cu-doped ZnO samples synthesized at 500°C, the PL spectrum shows a redshifted UV emission around 394 nm when excited at 320 nm using a xenon lamp. This is highlighted in Figure 4. This shift in the near-band-edge (NBE) emission indicates the formation of donor-bound excitons, confirming the successful incorporation of Cu into the ZnO lattice. The redshift compared to undoped ZnO is attributed to a reduction in the optical band gap due to Cu doping, in agreement with the XRD results that sho wed a decrease in crystallite size upon Cu incorporation. The Cu-doped ZnO sample with 5% Cu shows two dominant emissions: (i) UV emission at ~394 nm (NBE) (ii) Broad green emission centered around 524 nm. The green emission in Cu-doped ZnO has been explained by multiple models involving intrinsic and extrinsic defect states, including: Zinc vacancies, Oxygen vacancies, Interstitial zinc (Zn<sub>i</sub>) and oxygen (O<sub>i</sub>), Transitions between interstitial Zn and zinc vacancies, Substitutional Cu atoms acting as extrinsic impurities. Based on our experimental results and supporting literature, the green emission observed in the Cu-doped ZnO nanoparticles is primarily attributed to extrinsic defects introduced by Cu substitution at Zn sites. Simultaneously, point defects such as oxygen vacancies also contribute to this visible luminescence.

#### 3.3.3 Effect of Annealing Temperature on PL Emission at 700°C

PL spectra of Cu-doped ZnO nanoparticles synthesized at 700°C show an increase in both particle size and emission intensity. The UV emission band exhibits a redshift as the crystallite size increases, consistent with trends seen in UV–Visible absorption data. At elevated temperatures, the ZnO lattice experiences structural changes:

- Zinc interstitials (Zn<sub>i</sub>): These are more likely to ionize, contributing to electrical conductivity. However, their concentration decreases at higher temperatures due to possible Zn evaporation.
- Oxygen vacancies: These defects become more prevalent at higher annealing temperatures, leading to enhanced green luminescence.

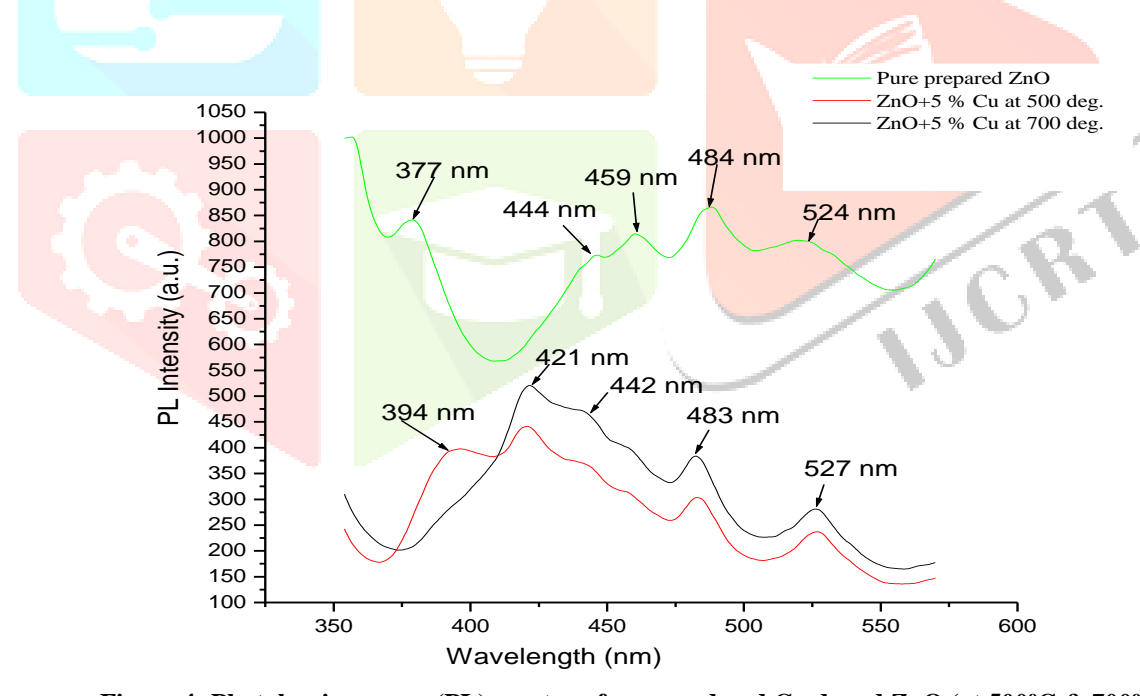


Figure 4: Photoluminescence (PL) spectra of prepared and Cu doped ZnO (at 500°C & 700°C)

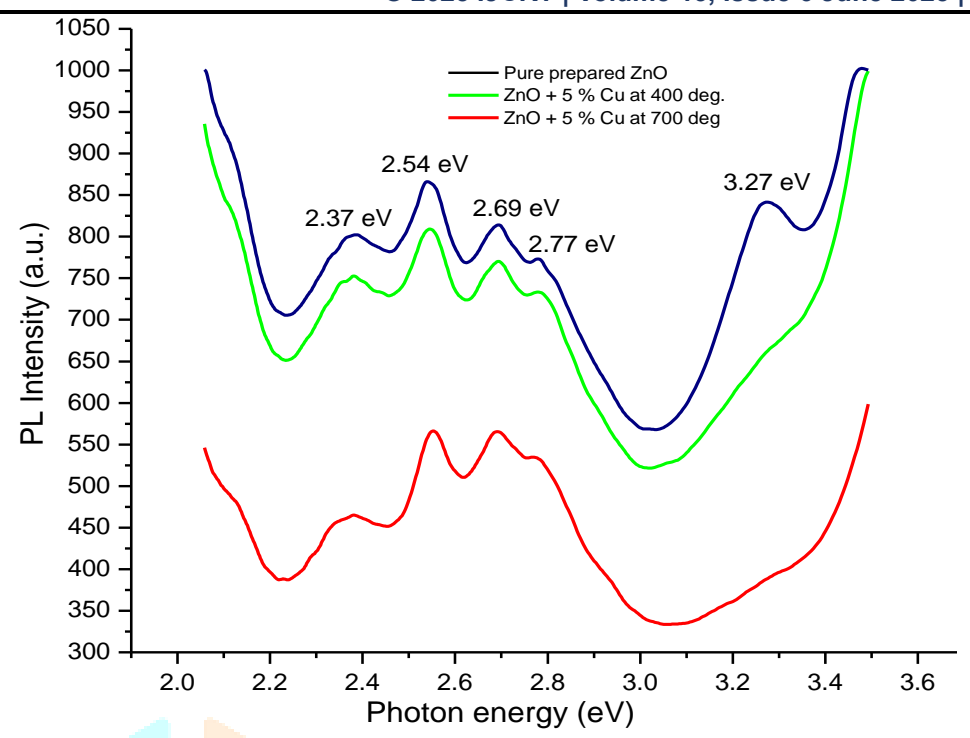


Figure 5: Photoluminescence (PL) spectra in term of photon energy of prepared ZnO and Cu doped ZnO nanoparticles at two different temperatures (500°C and 700°C)

Figure 5 shows the variation of the Photoluminescence (Pl) intensity versus photon energy curves for prepared pure ZnO nanoparticles and Cu doped ZnO nanoparticles synthesized at different annealing temperatures (500°C and 700°C).

# 3.3.4 UV-Visible spectra of prepared ZnO nanoparticles and Doped ZnO nanoparticles samples.

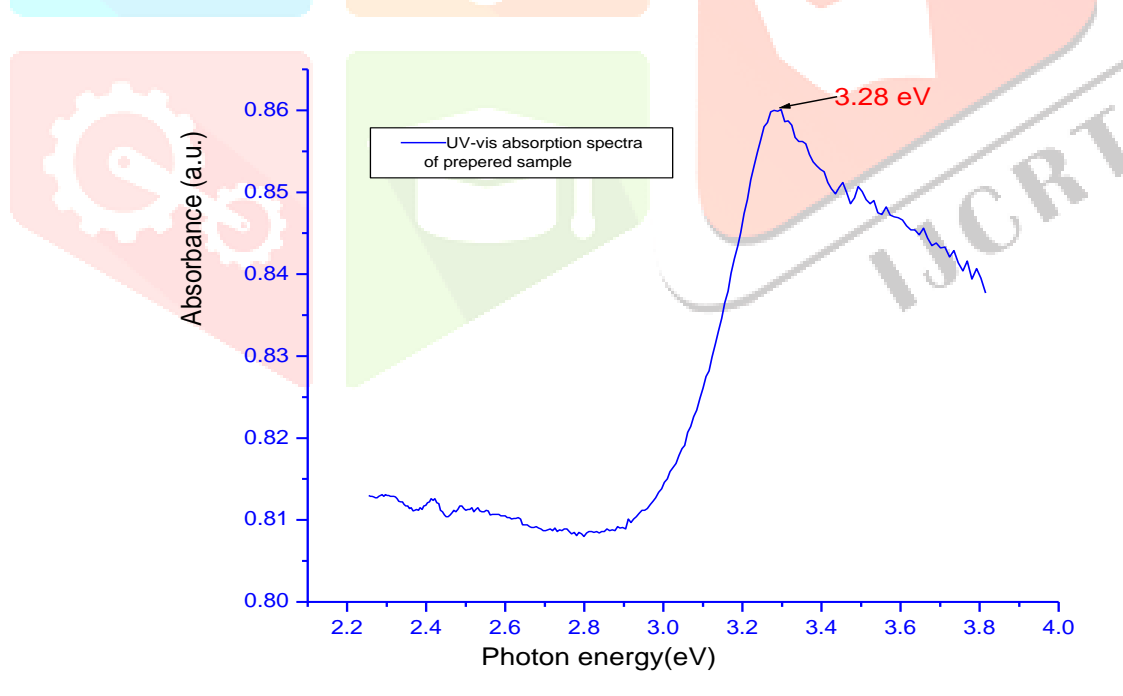


Figure 6: UV-visible absorption spectra of prepared pure ZnO nanoparticles

Figure 6 showed the UV-visible absorption spectra of prepared pure ZnO nanoparticles. Band gap energy, which is equal to the maximum peak absorption in the UV-visible absorption spectra was found to be equal to 3.28 eV as shown in figure (6)

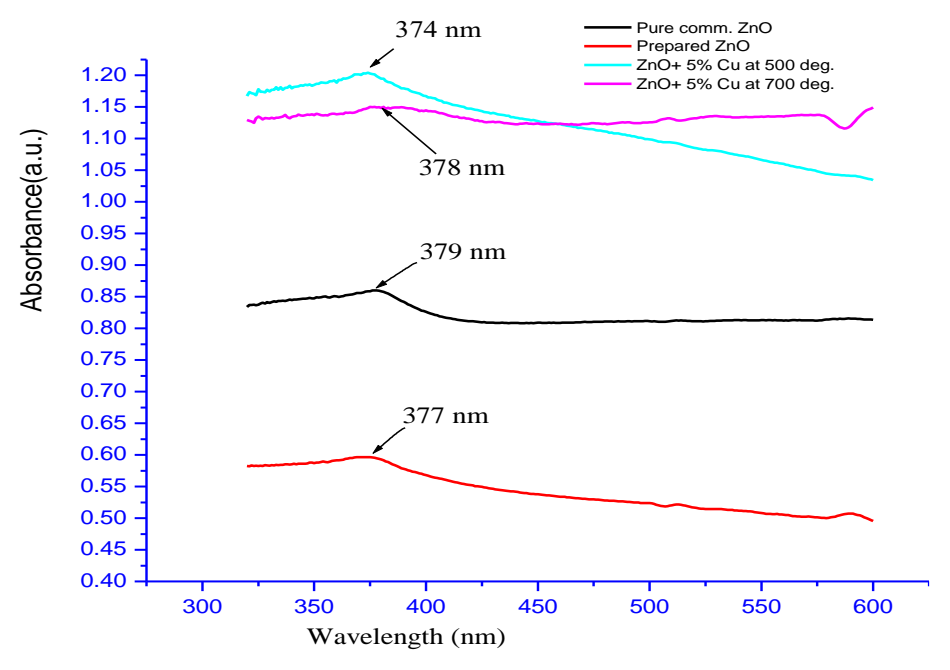


Figure 7: UV-visible absorption spectra of Commercial ZnO, Prepared pure ZnO, ZnO+5% Cu at 500°C and ZnO+ 5% Cu at 700°C nanoparticles.

The UV-visible absorption spectra of Cu-doped ZnO nanoparticles annealed at two different temperatures (500°C and 700°C) are presented in Figure (7). To enable a meaningful comparison, three sets of samples were analysed: commercial ZnO nanoparticles, laboratory-synthesized pure ZnO nanoparticles, and Cu-doped ZnO nanoparticles annealed at the aforementioned temperatures. The commercial ZnO sample was included as a reference to benchmark the absorption characteristics of the prepared samples. The optical band gap of the synthesized pure ZnO nanoparticles was found to be 3.27 eV, while the Cu-doped ZnO nanoparticles exhibited a slightly higher band gap of 3.31 eV. This increase in band gap upon doping can be attributed to the **Burstein–Moss effect**, wherein an increase in free carrier concentration—induced by copper incorporation—shifts the absorption edge to higher energies. With an increase in annealing temperature from 500°C to 700°C, a **redshift** in the optical absorption edge was observed, indicating a decrease in band gap from 3.31 eV to approximately 3.2–3.25 eV. This redshift is associated with the increase in crystallite size and improved crystalline quality at elevated temperatures. The band gap energy (Eg) was calculated using the standard relation:

 $Eg = hc / \lambda$ 

where h is Planck's constant, c is the speed of light, and  $\lambda$  is the absorption edge wavelength. The observed decrease in band gap with increasing temperature is primarily attributed to morphological enhancements and improved crystallinity of the Cu–ZnO nanoparticles. The reduction in the band gap energy reflects the shift of the absorption edge toward longer wavelengths, which signifies the narrowing of the band gap.

Additionally, improved crystallinity with increasing annealing temperature was evident, supporting the observed changes in optical behaviour. The overall reduction in Eg from 3.31 eV to 3.25 eV is therefore consistent with the enhanced crystalline nature of the material at higher annealing temperatures. These findings affirm that the optical band gap of Cu-doped ZnO nanoparticles is influenced significantly by both the doping effect and thermal treatment, with temperature playing a crucial role in modulating the structural and optical properties of the material.

# 4.Conclusion

In this study, pure and Cu-doped ZnO nanoparticles were successfully synthesized using the direct precipitation method and characterized structurally and optically. XRD analysis confirmed the formation of single-phase wurtzite ZnO without any secondary phases, indicating effective Cu incorporation into the ZnO lattice. A reduction in crystallite size upon doping and a slight expansion in lattice parameters supported the substitutional integration of Cu<sup>2+</sup> ions due to their larger ionic radius. SEM analyses revealed homogeneous morphology and confirmed the uniform distribution of Cu within the ZnO matrix. Photoluminescence studies demonstrated strong near-band-edge UV emission and visible emission bands, with green luminescence attributed to oxygen vacancies and Cu-related defects. Notably, Cu doping caused a redshift in the UV emission and an enhancement in green emission intensity, indicating an increase in defect-related transitions. UV-Visible spectroscopy revealed a band gap widening in Cu-doped ZnO due to the Burstein–Moss effect. However, with increasing annealing temperature, a redshift of the absorption edge was observed, indicating band gap narrowing, which was attributed to improved crystallinity and increased particle size. Overall, the results confirm that Cu doping and annealing temperature significantly influence the structural and optical properties of ZnO nanoparticles. These tuneable properties make Cu-doped ZnO a promising material for optoelectronic and photonic applications.

#### **References:**

- [1] D. Kumbhar et al., "Effect of Cu Doping on Structural and Optical Properties of ZnO Nanoparticles Using Sol–Gel Method," *Macromolecular Symposia*, vol. 387, no. 1, 2019. onlinelibrary.wiley.com
- [2] J. S. C. Licurgo et al., "Structural, electrical and optical properties of copper-doped zinc oxide films deposited by spray pyrolysis," *Cerâmica*, vol. 66, pp. 284–290, 2020.pubs.acs.org
- [3] J. H. Zheng et al., "Optical properties of Cu-doped ZnO nanoparticles experimental and first-principles theory research," *Journal of Materials Science: Materials in Electronics*, vol. 23, pp. 1521–1526, 2012. <a href="link.springer.com+1link.springer.com+1">link.springer.com+1</a>
- [4] L. Ben Saad et al., "Pure and Cu-Doped ZnO Nanoparticles: Hydrothermal Synthesis, Structural, and Optical Properties," *Russian Journal of Physical Chemistry A*, vol. 93, pp. 2782–2787, 2020.ui.adsabs.harvard.edu
- [5] I. L. Raj et al., "Effect of Cu2+ doping on the structural, optical, and vapor-sensing properties of ZnO thin films prepared by SILAR method," *Journal of Materials Science: Materials in Electronics*, vol. 31, pp. 1–10, 2020. link.springer.com
- [6] S. Iwan et al., "Morphology and optical properties of Cu–Al co-doped ZnO nanostructures," *Surfaces and Interfaces*, vol. 16, pp. 147–151, 2019.pubs.acs.org
- [7] A. P. Tarasov et al., "Effect of Ag, Cu, and Co Underlayers on Luminescence and Lasing of Vapor-Phase-Grown ZnO Microcrystals," in *Proceedings of the 2019 IEEE Conference on Advanced Optoelectronics and Lasers*, pp. 212–215, 2019.pubs.acs.org
- [8] A. Gaurav et al., "Study on the effect of copper ion doping in zinc oxide nanomaterials for photocatalytic applications," *Materials Chemistry and Physics*, vol. 230, pp. 162–171, 2019. pubs.acs.org
- [9] Q. Ma et al., "Cu doped ZnO hierarchical nanostructures: morphological evolution and photocatalytic property," *Journal of Materials Science: Materials in Electronics*, vol. 30, no. 3, pp. 2309–2315, 2019.pubs.acs.org+1link.springer.com+1
- [10] P. G. Undre et al., "Ferromagnetism in Cu2+ doped ZnO nanoparticles and their physical properties," *Science: Materials in Electronics*, vol. 30, no. 4, pp. 4014–4025, 2019. pubs. acs. org
- [11] O. Volnianska and P. Boguslawski, "Green luminescence and calculated optical properties of Cu ions in ZnO," *arXiv preprint arXiv:1911.02826*, 2019. arxiv.org
- [12] P. Samarasekara et al., "Impedance and electrical properties of Cu doped ZnO thin films," arXiv preprint arXiv:1703.02030, 2017.arxiv.org
- [13] A. K. Rana et al., "Enhancement of Two photon absorption with Ni doping in the dilute magnetic Semiconductor ZnO Crystalline Nanorods," *arXiv preprint arXiv:1708.09567*, 2017. arxiv.org
- [14] H. Liu et al., "Structural, optical and magnetic properties of Cu and V co-doped ZnO nanoparticles," *Physica E: Low-dimensional Systems and Nanostructures*, vol. 47, pp. 1–5, 2013. pubs.acs.org
- [15] A. Samavati et al., "Spectral features and antibacterial properties of Cu-doped ZnO nanoparticles prepared by sol-gel method," *Chinese Physics B*, vol. 25, no. 7, p. 077803, 2016. scientific.net
- [16] A. K. Sharma et al., "Synthesis of Doped Zinc Oxide Nanoparticles: A Review," *Materials Today: Proceedings*, vol. 11, part 2, pp. 767–775, 2019. sciencedirect.com
- [17] S. Valanarasu et al., "Role of solution pH on the microstructural properties of spin coated cobalt oxide thin films," *Journal of Nanosci. Nanotechnol.*, vol. 13, pp. 1–6, 2013.link.springer.com
- [18] P. Bharathi et al., "Growth and influence of Gd doping on ZnO nanostructures for enhanced optical, structural properties and gas sensing applications," *Applied Surface Science*, vol. 499, p. 143857, 2020.link.springer.com
- [19] K. Khojier, "Preparation and investigation of Al-doped ZnO thin films as a formaldehyde sensor with extremely low detection limit and considering the effect of RH," *Materials Science in Semiconductor Processing*, vol. 121, p. 105283, 2021.link.springer.com
- [20] S. Bilal, "Raman Spectrochemistry," in *Encyclopedia of Applied Electrochemistry*, Springer, New York, NY, 2014.scientific.net